



The Effect of Sail Layout on Fishing Vessels Hydrodynamics in the North Coast of Java using Computational Fluids Dynamic

Arif Winarno^{1,2}, Agung Sugeng Widodo^{1,*}, Gatot Ciptadi¹, Atiek Iriany¹

¹ Department of Environmental Science, postgraduate school, Brawijaya University, Malang, Indonesia

² Department of Marine Engineering, Hang Tuah University, Surabaya, Indonesia

ARTICLE INFO

Article history:

Received 31 May 2023

Received in revised form 25 June 2023

Accepted 19 July 2023

Available online 5 December 2023

Keywords:

Computational Fluids Dynamic (CFD);

Fishing Vessels; Resistance; Sail;

ABSTRACT

The fisheries sector is one of the potential sectors that contribute to Indonesia's state income, but it has often been neglected. Almost all fishing boats still use diesel engines as the main power source to propel the boat. The use of this type of fuel has an impact on increasing the level of air pollution such as CO₂, SO₂, and NO_x in the atmosphere. However, research to reduce ship pollution, especially the combination of propulsion system for fishing boats using engines and sails, is rarely carried out. This study aims to determine the hydrodynamic characteristics of fishing vessels on the north coast of Java due to the application of numerical variations in laying sails using Computational Fluids Dynamics (CFD). The numerical simulation results show that the placement of sails in each model variation results in a change in the fluid flow pattern from bow to stern which can contribute to fuel efficiency. From the comparison of the three models, the most effective placement of sails is at the bow of the ship.

1. Introduction

The fisheries sector is one of the potential sectors that contribute to Indonesia's state income, but it has often been neglected due to development of all state activities focusing on the land sector [1]. This is also marked by the number of fishing boats in Indonesia in 2019 showing the use of fishing boats without motors are only about 192,653 units, outboard motors about 427,309 units, motor boats about 316,287 units [2] when compared to other fish-producing countries such as China that has reached more than 1 million units of fishing vessels with catches reaching 61.7 million tons in 2013 [3].

Nevertheless, the fisheries sector remains as one of the largest sources of state revenue with a total production of 7.1 million tons with a production value of 170 trillion in 2020 [4]. In addition to the number of fishing boats in Indonesia which is still lacking, the use of adequate technology on

* Corresponding author.

E-mail address: agung_sw@ub.ac.id (Agung Sugeng Widodo)

fishing boats in Indonesia is also far from sophisticated and environmentally friendly. Almost all fishing boats still use diesel engines as the main power source to propel the ship. These fishing activities have an impact on increasing levels of air pollution such as Carbon dioxide (CO₂), Sulfur dioxide (SO₂), and nitrogen oxides (NO_x) in the atmosphere, especially on fishing vessels that use fossil-fuel diesel engines [5].

Numerical simulation research on ships and propulsion systems using Computational Fluids Dynamics (CFD) is often used for this. Permadi *et al.*, [6] conducted research on CFD simulation model for optimum design of B-Series propeller using multiple reference frame (MRF). Dani *et al.*, [7] researched about flow separation evaluation on tubercle ship propeller. Fitriadhy *et al.*, [8] have also conducted research on CFD prediction of b-series propeller performance in open water. Akkarachaiphant *et al.*, [9] have researched CFD Simulations operated by two stack vertical-axial wind turbines for high performance. Nabawi *et al.*, [10] have researched about study reduction of resistance on the flat hull ship of the semi-trimaran model: hull vane vs stern foil. Trimulyono *et al.*, [11] have researched about numerical simulation low filling ratio of sway sloshing in the prismatic tank using smoothed particle hydrodynamics. Daruis *et al.*, [12] researched CFD analysis of the heave and pitch motion of hull model. In addition, there are several other studies using CFD for ship objects [13-15].

Several previous studies regarding technical and economic analysis of the use of sails on fishing vessels to reduce emissions and save on fuel use have been discussed [16], and the results are that the calculation for operational costs has decreased by IDR 400,000 to IDR 900,000 per day. Furthermore, research on the study of the design of a sailing catamaran to obtain the optimum amount of resistance, stability, ship motion, and hydrostatic characteristics of the ship on the influence of the use of sails have been discussed [17], and the result is that the use of a triangular sail shape produces a maximum speed of up to 11.51 knots at 100° wind direction from the bow of the ship. The use of sails can reduce the operating power of the ship's engine by 69% [18]. Moreover, the additional force of wind power captured by the ship's sails can increase the speed of the ship by up to 0.5 knots [19]. The impact of these activities is one of the problems in Indonesia that is very important to find the solution so that fishing vessels operating in the Java Sea become fishing vessels that are environmentally friendly or low in emissions.

However, there has been no research on the combination of propulsion system for fishing boats using engines and sails, especially research on the effect of placing sails on the hydrodynamic characteristics of the ship. This study has three main objectives, namely first, to determine the effect of laying sails on a fishing boat model on the pattern of fluid flow on a fishing boat. Second, to determine the effect of laying the sails of a fishing boat model on the fluid velocity contour. Third, to know the smallest resistance force of the three variations. So that the lowest ship emission production is obtained. In addition, in this study a sail study was also carried out because the potential for wind around the Java Sea is very abundant due to the availability of energy with great intensity, such as wind speeds reaching 3.6 m/s.

2. Methodology

2.1 Ship Main Data

In this study, the laying of ship sails on fishing boats on the north coast of Java is based on total resistance, velocity contours, and flow distribution. For data collection, through previous research, this study is using the regression method in finding the main ship data [20]. After all the data were collected then a model can be done using Rhinoceros software and a simulation using ANSYS Fluent software. The simulation results from CFD are total vessel resistance, fluid flow velocity contours,

and fluid flow patterns. The fishing boat data used is the data obtained from past research [21], where the fishing boat operates in the North Coast area of Lamongan, East Java. The ship specifications are in more detail as shown in Table 1.

Table 1

Main data dimension

Principal dimension	Value
Length of the water line (LWL)	13.4 m
Height (D)	2.2 m
Breadth (B)	3 m
Draft (T)	1,27 m
Displacement	24,87 Ton
Block coefficient	0,508
Velocity speed	12 knots

The secondary sail data used is a triangular shaped sailing ship from the archipelago that operates in the Cirebon Sea [22] as shown in Figure 1. The selection of the type of sail shape is because according to Anwar *et al.*, [17] the contribution of the additional speed from the triangular sail is 4.4 knots or equal to 44%.

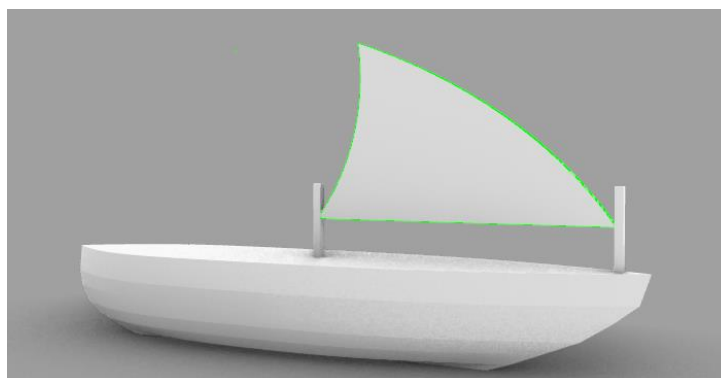


Fig. 1. Jenggolan Sail

2.2 Modeling

In this research, three different ship sail models were utilized, which are illustrated in Figure 2. The models are differentiated by the position of the sail on the ship, namely bow, midship, and stern. The Rhinoceros software was employed to create these models. The specifics of each model variation were carefully planned and executed.

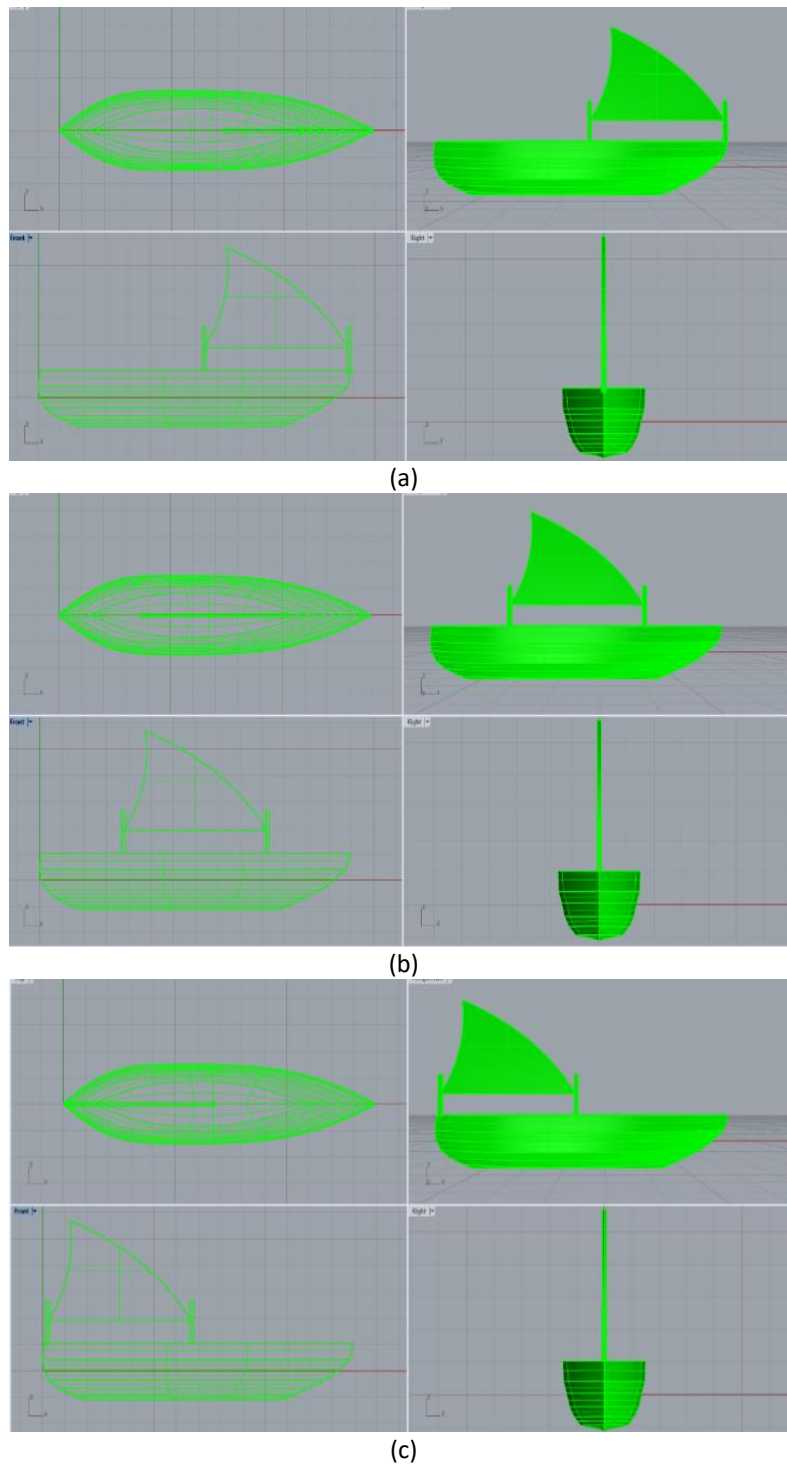


Fig. 2. Variation of the sails layout models: (a) Sail on the bow, (b) Sail on the midship, and (c) Sail on the stern

2.3 Computational Domain

The sailing ship model was represented as a fluid domain in the computational context, according to a previous study [23]. Figure 3 displays the boundaries of the computational grid, where the inlet-to-model distance is $3L$, the model-to-outlet distance is $4L$, the model-to-sidewall distance is $2.5L$, and the model-to-top-wall distance is $1L$. To be more specific, the length of the inlet-to-model

distance is 40.35 m, the model-to-outlet distance is 53.8 m, the model-to-sidewall distance is 33,625 m, the model-to-upstream distance is 13.45 m, and the model-to-downstream distance is 26.9 m.

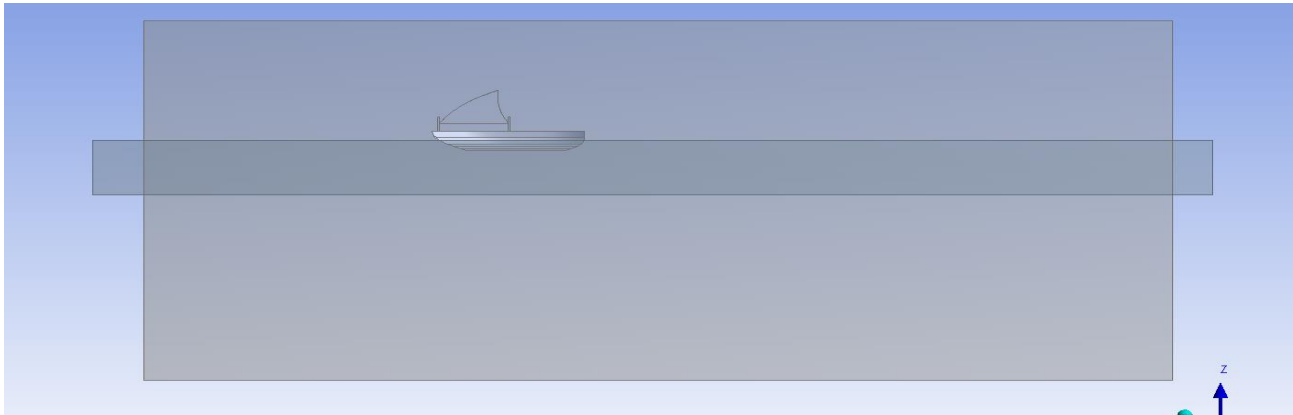


Fig. 3. Geometry

2.4 Meshing

The meshing process in CFD is an arrangement of components into small elements to determine the character of a ship shape to be analyzed. This involves discretizing a continuous fluid domain into a computational grid, enabling the solution of fluid equations through numerical methods [24]. Figure 4 illustrates the grid meshing process for ships and sails. An assembly mesh cut cell type was utilized, with a maximum inflation mesh of 10 layers to enhance the detail of the computational process.

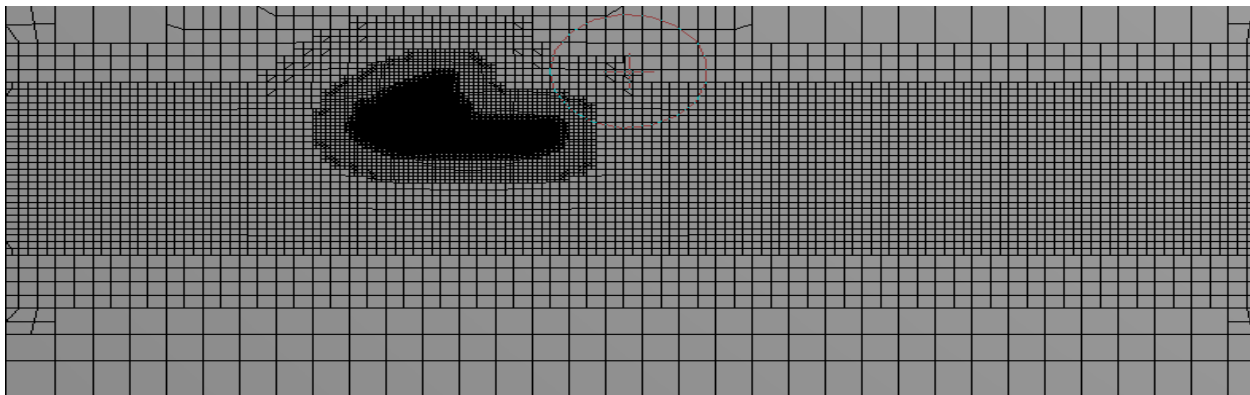


Fig. 4. Meshing

2.5 Computational Setup

Once the meshing process is finished, additional settings must be established in the setup stage to define boundary conditions for the CFD simulation. These parameters include fluid type, multiple types, cell zone condition, mesh interface, material, boundary condition, dynamic mesh, solution control, reference value, calculation activity, solution method, solution initialization, result settings, and last running calculation [25].

The models were tested at speeds ranging from 7 knots to 12 knots. In the initial setup, double-precision was used, along with two parallel processors and 2 Graphics Processing Units, with a stable type. The gravity acceleration on the z-axis was set to 9.81, and the standard k-epsilon turbulent model with two equations was employed. The multiphase standard used was an open channel flow and fluid volume was used for this study. The first phase was liquid air, while the second phase

consisted of liquid water. In terms of boundary conditions, the inlet pressure used a bottom level of -26.9 m, with speed varying accordingly. The pressure inlet type was multiphase. Simulation monitoring was conducted using plots, and the flat channel was employed for open channel usage. The run calculation employed a time scale factor of 0.5 and 1000 iterations. Figure 5 shows the simulation process monitoring.

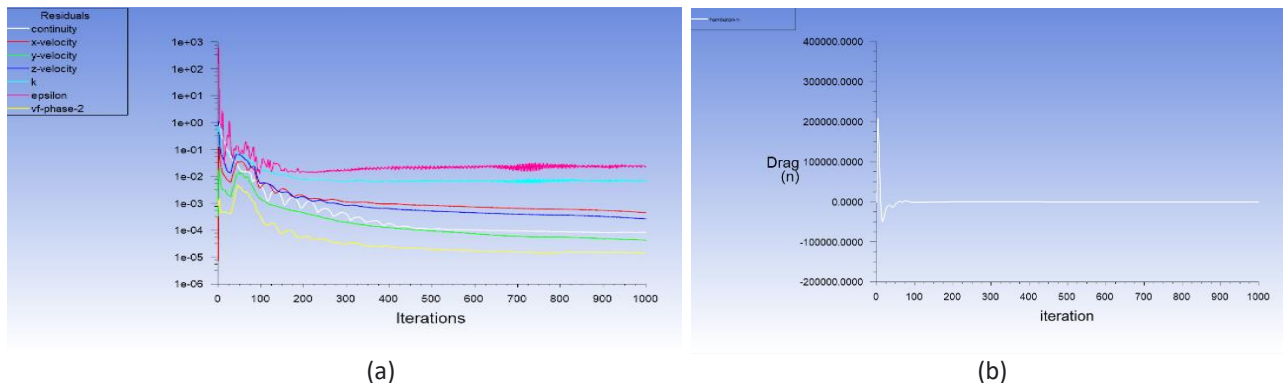


Fig. 5. Setup (a) iterations model (b) resistance model

Table 2 is a grid independence analysis. This is done to verify that the mesh size and type match this model and simulation. At the same speed and model, the simulation of four variations of mesh size were carried out. The first and second machine sizes produce a difference of around 8.09%. The first mesh has 1,846,943 cells and the second mesh has 982,375 cells.

Table 2

Grid independent

Velocity	Body sizing	Face sizing	Number of element	Drag (KN)
0.2572 m/s	40	20	1.846.943	0.2469
0.2572 m/s	50	25	982.375	0.2471
0.2572 m/s	60	30	604.470	0.1809
0.2572 m/s	65	32.5	744.824	0.1275

Validation of the accuracy of the results was carried out by comparing the results of the CFD and the results of running using the Maxsurf software. From table 3 it is known that the obstacles obtained from CFD are lower than the obstacles in the results of the Maxsurf obstacles with an average difference of 5% for each model variation. However, the difference is relatively small because it is under 6%.

Table 3

Resistance force comparison between CFD and Maxsurf

Model	Vs(m/s)	S(m ²)	ρ (kg/m ³)	Rt CFD(kN)	Rt Maxsurf (kN)	Selisih
Model 1	4,63	44,695	1,025	6,2483	6,4161	2.6 %
	6,1733	44,695	1,025	20,5995	21,432	4 %
Model 2	4,63	44,695	1,025	6,0442	6,1971	2.5 %
	6,1733	44,695	1,025	21,0982	22,2661	5,5 %
Model 3	4,63	44,695	1,025	6,3472	6,6518	4.7 %
	6,1733	44,695	1,025	21,7515	22,952	5.5 %

3. Result

3.1 Fluid Flow Velocity Contour

Figure 6 depicts the movement of fluid around the stern, hull, and bow of a model ship and sail traveling at a speed of 7 knots. The contours and colors in the figure represent the fluid flow's velocity and movement, with blue indicating low speed, green indicating medium speed, yellow indicating high speed, and red indicating very high speed.

The sail on the bow model has a green contour around the hull, with a fluid flow velocity of 3,247 m/s. At the bow, the flow velocity is 2,657 m/s, which increases to 2,952 m/s around the hull's sides before decreasing at the stern of the ship (Figure 6a). The midship sail type has a yellowish-green contour and a fluid flow velocity of 3,341 m/s. At the bow, the flow velocity is 3,063 m/s, which increases to 3,620 m/s around the hull's sides (Figure 6b). Finally, the sail type on the stern has a yellowish-green contour, with a fluid flow velocity of 3.035 m/s. At the bow, the flow velocity is 2.428 m/s, which increases to 2.731 m/s around the hull's sides (Figure 6c).

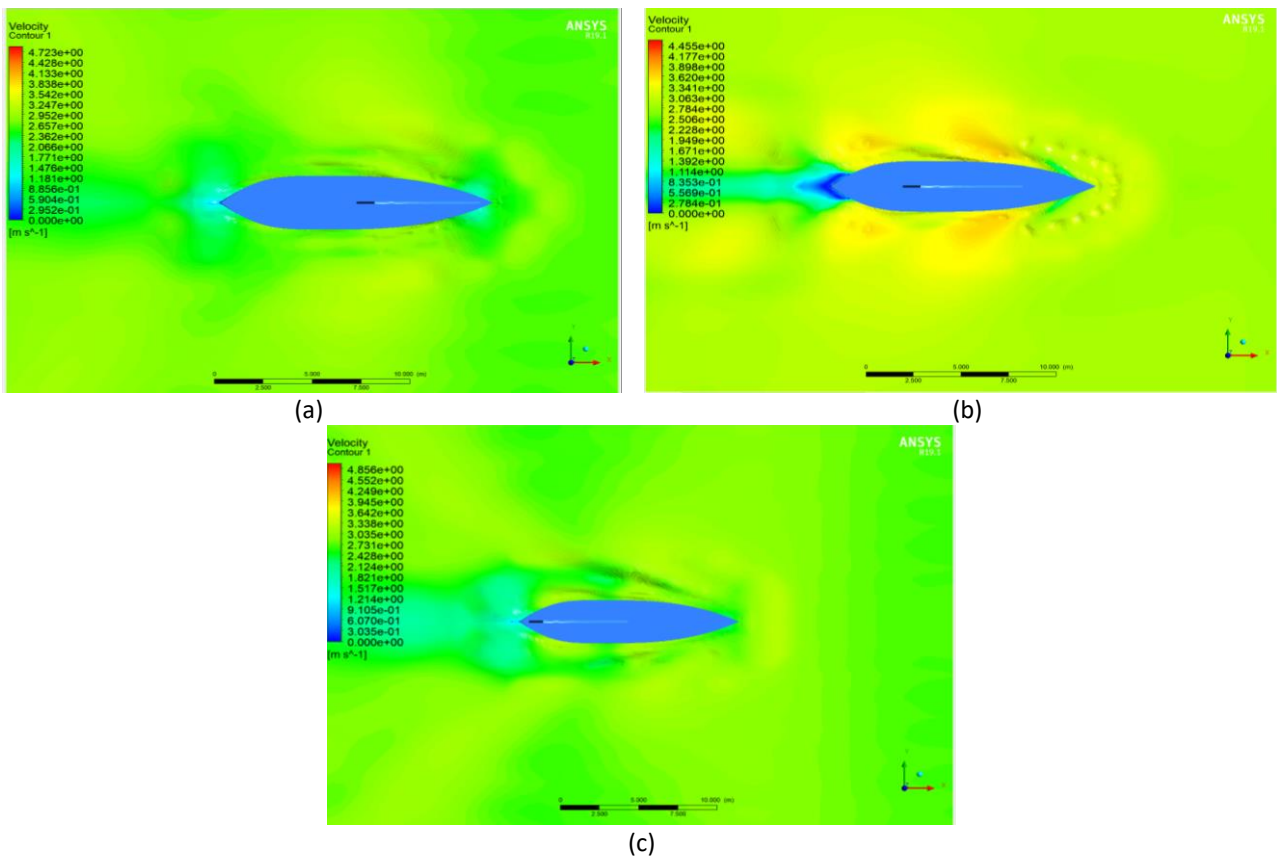


Fig. 6. Fluid flow velocity contour in 7 knots. (a) sail on the bow (b) sail on the midship (c) sail on the stern

Further after this is the contour of the fluid flow velocity in 8 knots speed for the ship models. The sail on bow type has a yellowish-green contour and the velocity of 3,638 m/s. The ship-bow flow velocity is 2,977 m/s, and the flow velocity at the hull side of the model is 3,308 m/s. Sail on the midship type has a yellowish-green contour and the velocity of the fluid flow on the sail area is 3,658 m/s. The ship-bow flow velocity is 3,353 m/s, and the flow velocity at the hull side of the model is 4,268 m/s. The sail on the stern type has a yellowish-green contour and the velocity of the fluid flow on the sail area is 3,711 m/s. The ship-bow flow velocity is 3,401 m/s, and the flow velocity at the model hull side is 3,062 m/s.

More after this is the contour of fluid flow velocity in 9 knots speed for the ship models. The sails on the bow type have a yellowish-green contour and the velocity around the sail of 0.1669 m/s. The ship-bow flow velocity is 0.667 m/s, and the flow velocity at the model hull side is 1.168 m/s. The midship-type sail also has a yellowish-green contour, and the velocity of the fluid flow on the sail area is 0.3302 m/s. The bow flow velocity of the ship is 0.825 m/s, and the flow velocity at the model hull side is 1.321 m/s. Finally, the stern-type sail also has a yellowish-green contour, and the velocity of the fluid flow on the sail area is 0.3489 m/s. The bow flow velocity of the ship is 0.8722 m/s, and the flow velocity at the model hull side is 1.570 m/s.

Furthermore, after this is the contour of fluid flow velocity at 10 knots speed for the ship models. The sails on the bow type are characterized by a yellowish-green contour around the hull, with a fluid flow velocity of 4,317 m/s. At the bow, the flow velocity is 3,238 m/s, which increases on the sides of the hull to 4,677 m/s and then decreases at the stern of the ship. The sail on the midship type has a yellowish-green contour. This model has a fluid flow velocity of 4,140 m/s. Hence, the bow flow velocity is 4,491 m/s and increases on the hull surface area by 4,837 m/s. The color contour of the sail type on the stern is yellowish green. This model has a fluid flow velocity of 4,541 m/s. The bow flow velocity was 4,192 m/s, then increased on the side of the hull to 5,240 m/s.

After this is the contour of the fluid flow in 11 knots speed on the ship models. The sails on this bow have a reddish-yellow contour around the hull which indicates that the velocity is 5,016 m/s. However, the bow flow velocity is 4,229 m/s, then increases on the sides of the hull to 5,374 m/s and descends at the stern of the ship. The sail on the midship type has a yellowish-green contour. This model has a fluid flow velocity of 4,655 m/s. Hence, the bow fluid flow velocity is 5,043 m/s and descends around the hull to 4,655 m/s. The color contour of the sail type on the stern is yellowish green. This model has a fluid flow velocity of 4,245 m/s. The bow fluid flow velocity was 3,859 m/s, then increased around the side of the hull to 4,631 m/s.

Finally, after this is the contour of fluid flow contours in 12 knots speed for the models as in depicted in Figure 7. The sails on this bow have a reddish-orange contour which has a fluid flow velocity of 4,919 m/s. However, the bow fluid flow velocity is 5,329 m/s, then increases on the sides of the hull to 6,149 m/s and descends at the stern of the ship (Figure 7a). The sail on the midship type has a reddish-orange contour. This model has a fluid flow velocity of 5,364 m/s. Hence, the bow fluid flow velocity is 5,776 m/s and increases on the hull surface area by 6,189 m/s (Figure 7b). The color contour of the sail type on the stern is reddish orange. This model has a fluid flow velocity of 6.142 m/s. The bow fluid flow velocity was 5,323 m/s, then increased on the side of the hull to 5,732 m/s (Figure 7c).

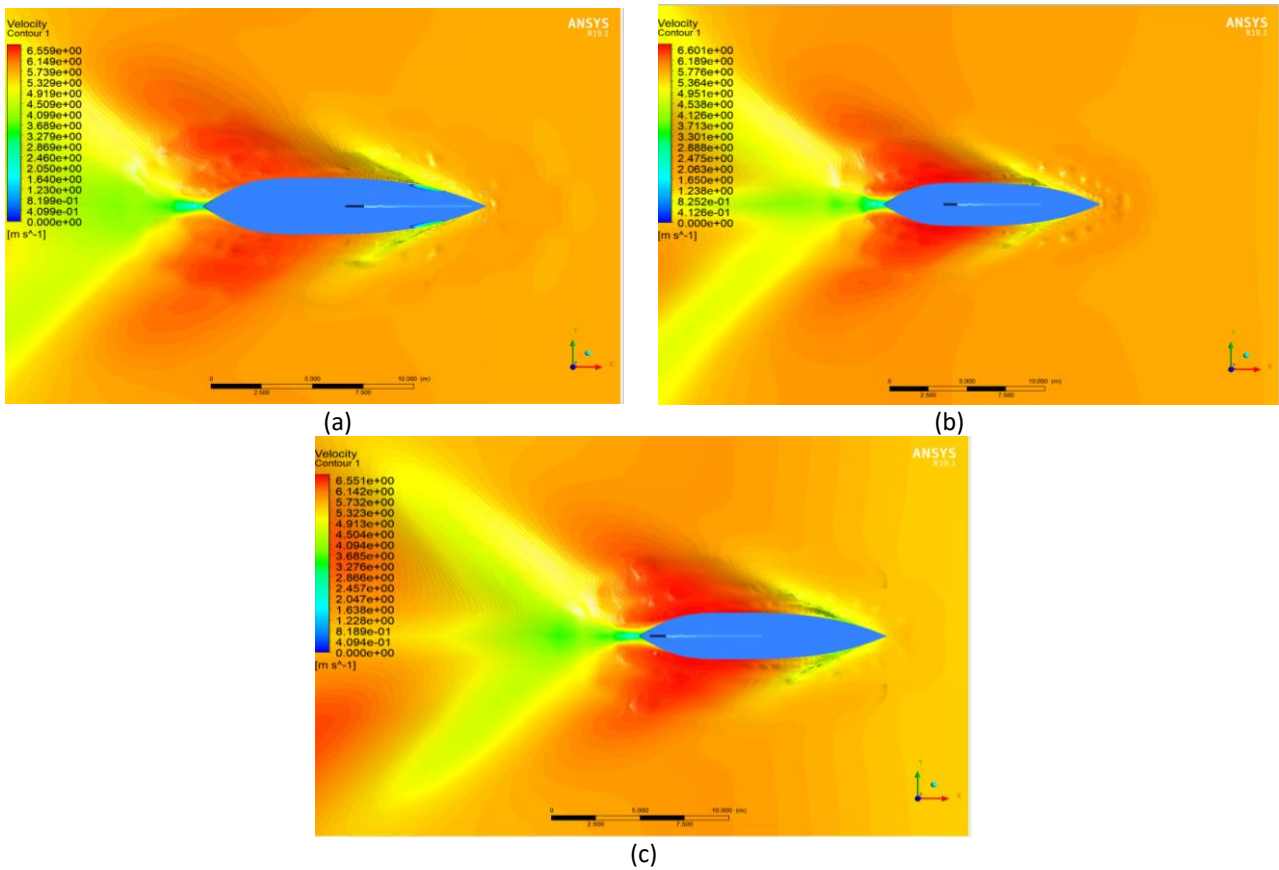


Fig. 7. Fluid flow velocity contour in 12 knots (a) sail on the bow (b) sail on midship (c) sail on the stern

All models show almost the same speed pattern. The results of the velocity contour analysis show that the influence of the placement of the sail on each variation of the model results in a difference in the velocity contour. The midship to the stern has the highest speed compared to other parts of the ship. As an example, at a speed of 12 knots, each model gets an additional speed where the sail on the bow gets an additional speed of 6.2%, the sail on the midship gets an additional speed of 6.9%, and the sail on the stern gets an additional speed of 6.3%. There is an additional speed of each variation of the model getting an additional speed of up to 6.9%.

3.2 Fluid Flow Pattern

This study also observed the fluid flow pattern around ship models and found that it consists of vectors and flow lines. The flow lines represent the path of the fluid on the model water's surface, while the vectors indicate the direction of the fluid flow. The fluid flow patterns for three ship models (sail on the bow, sail on midship, and sail on the stern) at 7 knots are presented in Figure 8.

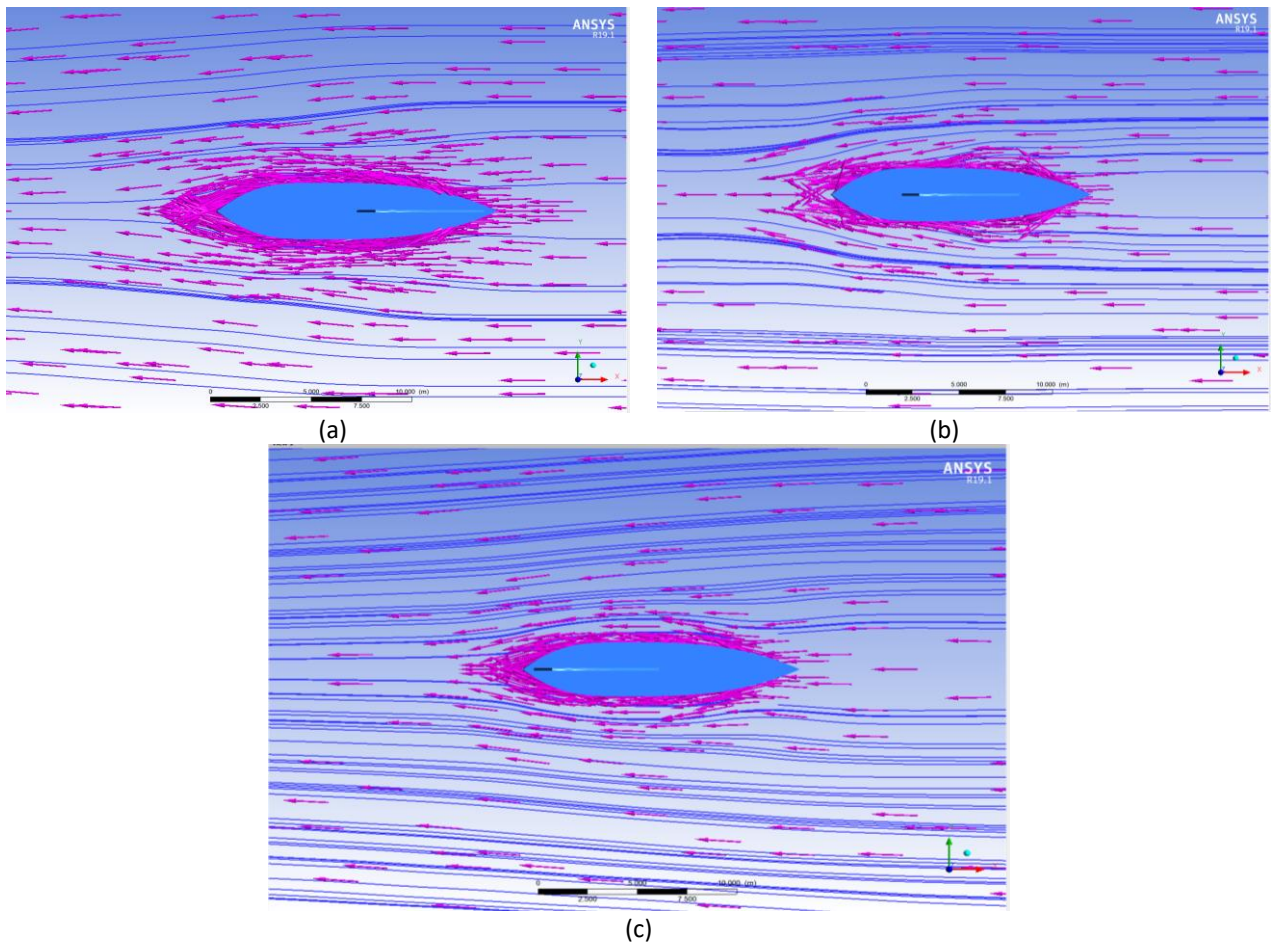


Fig. 8. Fluid flow pattern in 7 knots (a) sail on the bow (b) sail on the midship (c) sail on the stern

Figure 8 depicts the fluid flow patterns of three different ship models in 7 knots. The bow sail displays a straight and turbulent flow, narrowing behind the stern of the vessel due to changes in the flow direction. The midship sail also narrows behind the stern but straightens after that point. The stern sails exhibit a straight and wavy flow from bow to stern. Notably, all three models display a turbulent flow pattern behind the ship, consistent with their respective Reynolds numbers.

As for the fluid flow patterns of the ship models at 8 knots and 9 knots, the sail on the bow of the ship shows a straight flow pattern that narrows towards the stern for both speeds. The midship sail exhibits a straight and irregular flow pattern from the bow to the stern for both speeds as well. On the other hand, the sail at the stern has a straight flow pattern towards the midship that becomes wavy towards the rear for 8 knots and narrows to the rear for 9 knots. All models demonstrate a turbulent flow pattern behind the ship that corresponds to the Reynolds number for each model.

The fluid flow pattern for the ship model at 10 knots illustrates that the sail on the bow has a straight and narrow flow direction towards the rear of the ship, and it becomes wavy at the rear of the vessel. Meanwhile, the sail in the midship has a straight flow direction and widens on the hull. It becomes wavy from the bow to the rear of the ship. Finally, the sails at the stern have a flow pattern that is straight to the rear of the ship and wavy to the rear of the ship

The pattern of the fluid flow in 11 knots for the model ship is shown [next](#). The sails on this bow have straight and wavy flow directions behind the ship. The sail in the midship has a straight and wide current direction on the hull and is wavy at the rear of the ship. The sails at the stern have a stream that is straight and wide to the side of the hull and wavy to the rear of the ship.

Figure 9 illustrates the fluid flow pattern in 12 knots for the model ship. The bow sail exhibits a straight and irregularly wavy flow pattern from the bow to the rear of the ship (Figure 9a). The midship sail shows a straight current pattern with irregular waves on the hull (Figure 9b). The stern sails exhibit a straight and wide stream that narrows towards the rear of the ship (Figure 9c).

All models show almost the same flow pattern. The analysis of the fluid flow patterns demonstrates that the placement of the sail on each model variation alters the steady flow at the bow, resulting in changes in the flow pattern towards the stern. The Reynolds number calculation indicates that all three models experience turbulence at the stern.

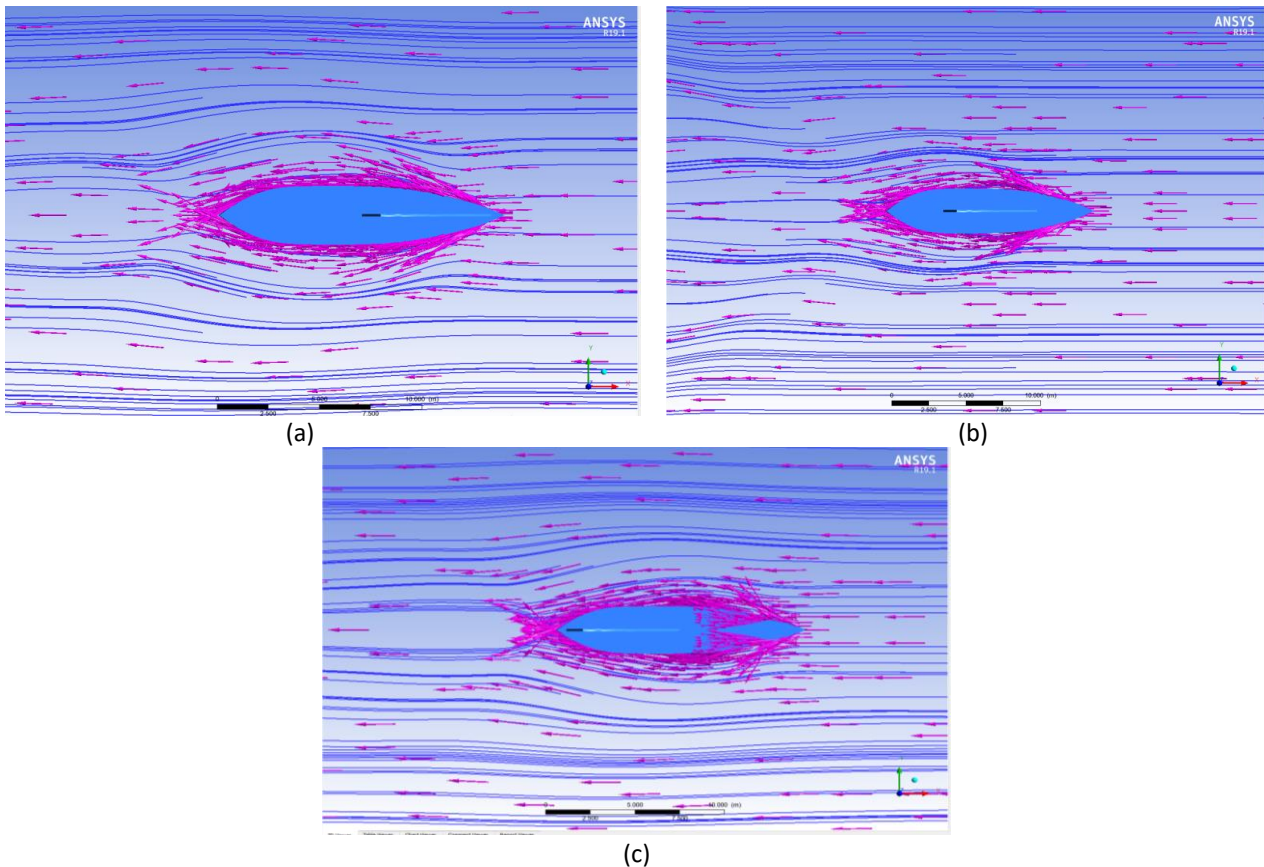


Fig. 9. Fluid flow pattern in 12 knots (a) sail on the bow (b) sail on the midship (c) sail on the stern

3.3 Resistance Force

The tables showing the resistance force on the sails for each model are presented in Tables 4, 5, and 6 for the bow, midship, and stern respectively. The speed variations tested were 7 knots, 8 knots, 9 knots, 10 knots, 11 knots, and 12 knots, and a body sizing of 0.6 m and a face sizing of 0.1 m were used for the calculations. The mesh sizing used was faced sizing for the ship and sail models, and body sizing for other domains.

Table 4

Sail on bow resistance

Speed (Knot)	Face sizing (m)	Body sizing (m)	Element	Inflation	Resistance (N)
7	01	06	354790	10	1433.289
8	01	06	354790	10	2158.143
9	01	06	354790	10	4548.334
10	01	06	354790	10	6985.691
11	01	06	354790	10	14463.455
12	01	06	354790	10	20599.574

Table 5

Sail on midship resistance

Speed (Knot)	Face sizing (m)	Body sizing (m)	Element	Inflation	Resistance (N)
7	01	06	394054	10	1647.329
8	01	06	394054	10	2402.785
9	01	06	394054	10	5161.334
10	01	06	394054	10	7198.771
11	01	06	394054	10	17997.521
12	01	06	394054	10	21098.252

Table 6

Sail on stern resistance

Speed (Knot)	Face sizing (m)	Body sizing (m)	Element	Inflation	Resistance (N)
7	01	06	330656	10	1797.619
8	01	06	330656	10	2591.421
9	01	06	330656	10	5441.798
10	01	06	330656	10	7312.661
11	01	06	330656	10	18146.359
12	01	06	330656	10	21751.556

The numerical calculations indicate that the position of the sails has a considerable impact on the resistance of the ship. By comparing the three tables, it is apparent that the resistance increases following an increase in the model's speed. The resistance force is observed to be lowest for the sail at the bow, followed by the sail in the midship, and the sail at the stern, in order of increasing magnitude.

4. Conclusions

In this study, Information about the effect of sail layout on the hydrodynamics of fishing vessels is found to be still rarely studied. The selection of the location of the sail that is suitable for the needs of the hybrid propulsion system greatly affects the magnitude of the resistance. The variation of speed on each model is 7 knots, 8 knots, 9 knots, 10 knots, 11 knots, and 12 knots. The results show the three model's comparison gets an additional speed of up to 6.2% and the most effective laying of the sail is on the bow of the ship. Then, thr resistance force is observed to be lowest for the sail at the bow, followed by the sail in the midship, and the sail at the stern. Further research can be carried out by conducting experimental research to validate this research, besides that research on different screen shapes can also be carried out to perfect this research. Furthermore, the next research can also includes wind and current factors in the research object.

Acknowledgements

We would like to express our gratitude to Hang Tuah University Surabaya for providing financial support for this research. We also extend our thanks to the fluid laboratory team for their support and for providing the facilities for conducting this research.

References

- [1] Iqbal, Muhammad, and Wasis Dwi Aryawan. "Desain Kapal Ikan Hibrida Berbahan Dasar High Density Polyethylene sebagai Penunjang Potensi Laut Provinsi Kepulauan Riau." *Jurnal Teknik ITS* 8, no. 2 (2019): G159-G165. <https://doi.org/10.12962/j23373539.v8i2.43943>
- [2] KKP. (2021). Jumlah Kapal Menurut Provinsi dan Jenis Penangkapan. https://statistik.kkp.go.id/home.php?m=prod_ikan_prov&i=2#panel-footer, 2021. .
- [3] FAO. The state of world fisheries and aquaculture—meeting the sustainable development goals. (2018).
- [4] BPS. Produksi Perikanan Tangkap Menurut Provinsi dan Jenis Penangkapan. (2021). www.bps.go.id.
- [5] Korol, I., & Latorre, R. Development of Eco-Friendly Fishing Vessel An ecological vehicle powered by renewable energy. (2010). EVER Monaco.
- [6] Permadi, Niki Veranda Agil, and Erik Sugianto. "CFD Simulation Model for Optimum Design of B-Series Propeller using Multiple Reference Frame (MRF)." *CFD Letters* 14, no. 11 (2022): 22-39. <https://doi.org/10.37934/cfdl.14.11.2239>
- [7] Arifin, Mohammad Danil, Frengki Mohamad Felayati, and Andi Haris Muhammad. "Flow Separation Evaluation on Tubercle Ship Propeller." *CFD Letters* 14, no. 4 (2022): 43-50. <https://doi.org/10.37934/cfdl.14.4.4350>
- [8] Fitriadhy, Ahmad, Nur Amira Adam, C. J. Quah, Jaswar Koto, and Faisal Mahmuddin. "CFD prediction of b-series propeller performance in open water." *CFD letters* 12, no. 2 (2020): 58-68. <https://doi.org/10.37934/cfdl.14.4.4350>
- [9] Akkarachaiphant, Thanaphat, Boonyarit Chatthong, Yutthana Tirawanichakul, and Montri Luengchavanon. "CFD Simulations Operated by Two Stack Vertical-Axial Wind Turbines for High Performance." *CFD Letters* 14, no. 3 (2022): 1-10. <https://doi.org/10.37934/cfdl.14.3.110>
- [10] Nabawi, Rahmat Azis. "Study Reduction of Resistance on The Flat Hull Ship of The Semi-Trimaran Model: Hull Vane Vs Stern Foil." *CFD Letters* 13, no. 12 (2021): 32-44. <https://doi.org/10.37934/cfdl.13.12.3244>
- [11] Trimulyono, Andi, Deddy Chrismiando, Haikal Atthariq, and Samuel Samuel. "Numerical Simulation Low Filling Ratio of Sway Sloshing in the Prismatic Tank Using Smoothed Particle Hydrodynamics." *CFD Letters* 14, no. 7 (2022): 113-123. <https://doi.org/10.37934/cfdl.14.7.113123>
- [12] Rocha Filho, Sergio Murilo Daruis, Roger Matsumoto Moreira, Marcio Zamboti Fortes, and Rafael Eitor dos Santos. "CFD Analysis of The Heave and Pitch Motion of Hull Model." *CFD Letters* 14, no. 4 (2022): 14-31. <https://doi.org/10.37934/cfdl.14.4.1431>
- [13] Sugianto, Erik, Jeng-Horng Chen, and Niki Veranda Agil Permadi. "Effect of monohull type and catamaran hull type on ocean waste collection behavior using OpenFOAM." *Water* 14, no. 17 (2022): 2623. <https://doi.org/10.3390/w14172623>
- [14] Sugianto, Erik, Arif Winarno, Ratna Indriyani, and Jeng Horng Chen. "Hull Number Effect in Ship Using Conveyor on Ocean Waste Collection." *Kapal: Jurnal Ilmu Pengetahuan dan Teknologi Kelautan* 18, no. 3 (2021): 128-139. <https://doi.org/10.14710/kapal.v18i3.40744>
- [15] Permadi, N. V. A., J. H. Chen, and E. Sugianto. "Influence of Full and Symmetrical Domains on the Numerical Flow around a SUBOFF Submarine Model using OpenFOAM." *Journal of Applied Fluid Mechanics* 16, no. 5 (2023): 1017-1029. <https://doi.org/10.47176/jafm.16.05.1513>
- [16] Hafiz, Wahdani Naufal, and Pramudya Imawan Santosa. "STUDI PERANCANGAN KAPAL IKAN DENGAN PEMANFAATAN ENERGI TERBARUKAN BERBASIS TENAGA ANGIN DAN TENAGA SURYA UNTUK KEPULAUAN MOROTAI." *Jurnal Sumberdaya Bumi Berkelanjutan (SEMATAN)* 3, no. 1 (2021): 146-154.
- [17] Anwar, M. Ulil, Andi Trimulyono, and Muhammad Iqbal. "Studi Perancangan Desain layar Berbasis Cfd Pada Perahu Motor Tempel Tipe Katir Di Pelabuhan Sadeng Guna Penghematan Bbm." *Jurnal Teknik Perkapalan* 4, no. 1 (2016).
- [18] Hadi, Eko Sasmito, Ari Wibawa, and Andhi Kusuma. "Perancangan Kapal Wisata Katamaran Dengan Sistem Penggerak Mesin Dan Layar Di Daerah Wisata Bahari Bareleng (Batam, Rempang, Galang)." *Kapal: Jurnal Ilmu Pengetahuan dan Teknologi Kelautan* 9, no. 1: 14-23.
- [19] Fadillah, A., Ibrahim, B. K. A., Manullang, S., Rizky, I., & Putra, P. Penerapan Renewable Energy Pada Kapal Wisata Jenis Pinisi. Seminar MASTER PPNS. Vol. 4. No. 1. (2019).
- [20] Aldás, Paúl Sebastián Dávila, *et al.*, "Monohull ship hydrodynamic simulation using CFD." *International Journal of Mathematics in Operational Research* 15.4 (2019): 417-433. doi: 10.1504/IJMOR.2019.103000. <https://doi.org/10.1504/IJMOR.2019.103000>
- [21] Arif Budi Utomo. Optimasi bentuk lambung kapal ikan tradisional di desa kranji kabupaten lamongan dengan

- metode b-spline surfaces. Universitas Hangtuh Surabaya (2021).
- [22] Yanuar Al fiqri. Teknologi Perkapalan Nusantara Abad Ke-16 - 18 Masehi. *Jurnal Sejarah, Budaya, dan Pengajarannya*, vol. 14 (1) (2019): 1–21,. <http://dx.doi.org/10.17977/um020v14i12020p1-21>.
<https://doi.org/10.17977/um020v14i12020p1-21>
- [23] ITTC. Practical Guidelines for Ship CFD Applications. In ITTC—Recommended Procedures and Guidelines; 26th ITTC Executive Committee: Rio de Janeiro, Brazil, vol. Chapter 7 (2011).
- [24] Sugianto, Erik, Arif Winarno, Ratna Indriyani, and Jeng Horng Chen. "Hull Number Effect in Ship Using Conveyor on Ocean Waste Collection." *Kapal: Jurnal Ilmu Pengetahuan dan Teknologi Kelautan* 18, no. 3 (2021): 128-139.
<https://doi.org/10.14710/kapal.v18i3.40744>
- [25] Febyan Pradana. Analisa Tahanan Model dan Simulasi Computational Fluid Dynamic pada Kapal Pembersih Sampah Laut dengan Variasi Tipe Lambung Monohull di Pesisir Perairan Surabaya. Universitas Hangtuh Surabaya. (2021).